Supporting Information: Contributions to regional precipitation change and its polar-amplified pattern under warming

David B. Bonan[1], Nicole Feldl[2], Mark D. Zelinka[3], Lily C. Hahn[4]

[1]Environmental Science and Engineering, California Institute of Technology, Pasadena, CA, USA
[2]Earth and Planetary Sciences, University of California Santa Cruz, CA, USA
[3]Lawrence Livermore National Laboratory, Livermore, CA, USA
[4]Department of Atmospheric Sciences, University of Washington, Seattle, WA, USA

June 20, 2023

Table of Contents

	Model Name	Ensemble
1.	ACCESS1-0	r1i1p1
2.	ACCESS1-3	r1i1p1
3.	bcc-csm1-1	r1i1p1
4.	bcc-csm1-1-m	r1i1p1
5.	BNU-ESM	r1i1p1
6.	CanESM2	r1i1p1
7.	CCSM4	r1i1p1
8.	CNRM-CM5	r1i1p1
9.	CNRM-CM5-2	r1i1p1
10.	GFDL-CM3	r1i1p1
11.	GFDL-ESM2G	r1i1p1
12.	GFDL-ESM2G-1	r1i1p1
13.	GFDL-ESM2M	r1i1p1
14.	GISS-E2-H	r1i1p1
15.	GISS-E2-R	r1i1p1
16.	HadGEM2-ES	r1i1p1
17.	IPSL-CM5A-LR	r1i1p1
18.	IPSL-CM5A-MR	r1i1p1
19.	IPSL-CM5B-LR	r1i1p1
20.	MIROC5	r1i1p1
21.	MIROC-ESM	r1i1p1
22.	MRI-CGCM3	r1i1p1
23.	NorESM1-M	r1i1p1

Supplemental Table 1: List of the CMIP5 coupled GCMs ($n = 23$) used in this study. The abrupt-4xCO2 simulation for each GCM is used.

	Model Name	Ensemble
1.	ACCESS-CM2	r1i1p1f1
2.	ACCESS-ESM1-5	r1i1p1f1, r2i1p1f1
3.	AWI-CM-1-1MR	r1i1p1f1
4.	BCC-CSM2-MR	r1i1p1f1
5.	CESM2	r1i1p1f1
6.	CESM2-FV2	r1i1p1f1
7.	CESM2-WACCM	r1i1p1f1
8.	CESM2-WACCM-Fv2	r1i1p1f1
9.	CMCC-CM2-SR5	r1i1p1f1
10.	CMCC-ESM2	r1i1p1f1
11.	CMCC-CM2-HR4	r1i1p1f1
12.	CNRM-CM6-1	r1i1p1f2
13.	CNRM-CM6-1-HR	r1i1p1f2
14.	CNRM-ESM2-1	r1i1p1f2, r2i1p1f2, r3i1p1f2
15.	CanESM5	r1i1p1f1, r1i1p2f1
16.	CanESM5-1	r1i1p1f1, r1i1p2f1
17.	E3SM-1-0	r1i1p1f1
18.	E3SM-2-0	r1i1p1f1, r2i1p1f1
19.	EC-Earth3	r3i1p1f1, r8i1p1f1
20.	EC-Earth3-CC	r1i1p1f1
21.	EC-Earth3-Veg-LR	r1i1p1f1
22.	EC-Earth3-Veg	r1i1p1f1
23.	FGOALS-f3-L	r1i1p1f1, r2i1p1f1, r3i1p1f1
24.	FGOALS-g3	r1i1p1f1
25.	GFDL-CM4	r1i1p1f1
26.	GISS-E2-1-H	r1i1p1f1, r1i1p3f1, r1i1p5f1
27.	GISS-E2-2-H	r1i1p1f1
28.	HadGEm3-GC31-LL	r1i1p1f3
29.	HadGEm3-GC31-MM	r1i1p1f3
30.	IITM-ESM	r1i1p1f1
31.	INM-CM4-8	r1i1p1f1
32.	INM-CM5-0	r1i1p1f1
33.	IPSL-CM6A-LR	r1i1p1f1
34.	IPSL-CM6A-LR-INCA	r1i1p1f1
35.	KACE-1-0-G	r1i1p1f1
36.	MIROC-ES2H	r1i1p4f2, r2i1p4f2, r3i1p4f2
37.	MIROC-ES2L	r1i1p1f2
38.	MIROC6	r1i1p1f1
39.	MPI-ESM-1-2-HAM	r1i1p1f1
40.	MPI-ESM1-2-HR	r1i1p1f1
41.	MPI-ESM1-2-LR	r1i1p1f1
42.	MRI-ESM2-0	r1i1p1f1, r1i2p1f1, r4i1p1f1, r7i1p1f1, r10i1p1f1, r13i1p1f1
43.	UKESM1-0-LL	r1i1p1f2

Supplemental Table 2: List of the CMIP6 coupled GCMs ($n = 61$) used in this study. The abrupt-4xCO2 simulation for each GCM is used.

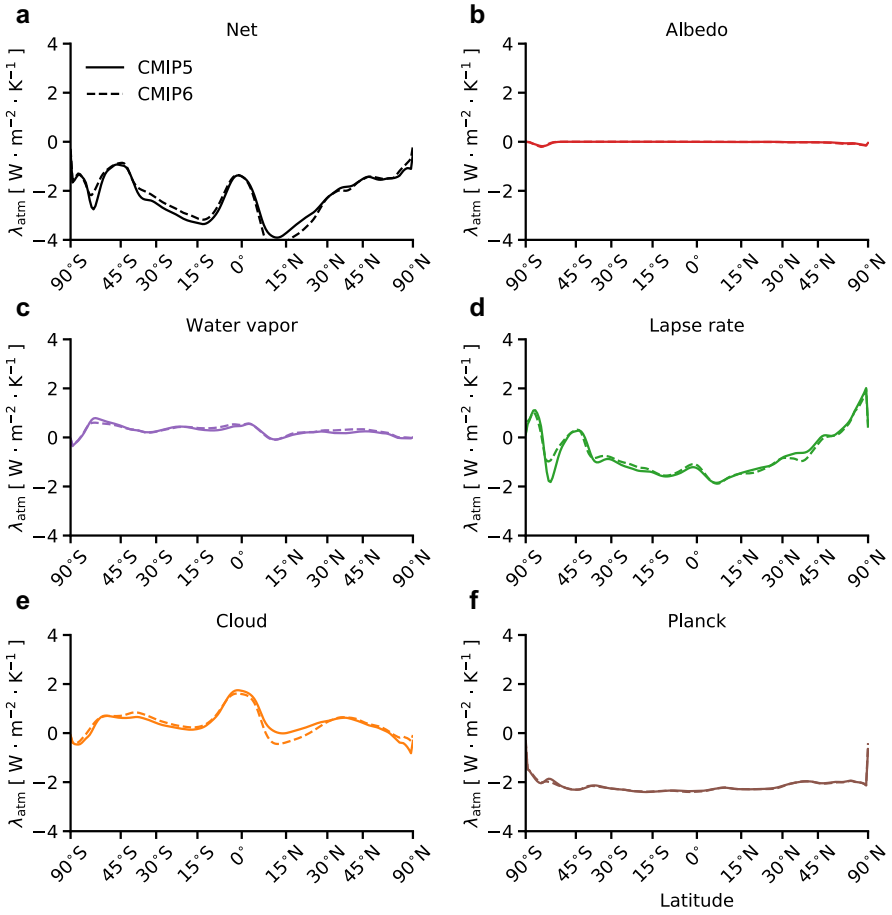

Supplemental Figure 1: **Zonal-mean local atmospheric radiative feedbacks in CMIP5 and CMIP6.** The zonal-mean and multi-model mean (a) net, (b) surface-albedo, (c) water vapor, (d) lapse rate, (e) cloud, and (f) Planck atmospheric radiative feedbacks for CMIP5 (solid line) and CMIP6 (dashed line). Each feedback is normalized by the local temperature change and calculated as the difference between top-of-atmosphere and surface radiative feedbacks.

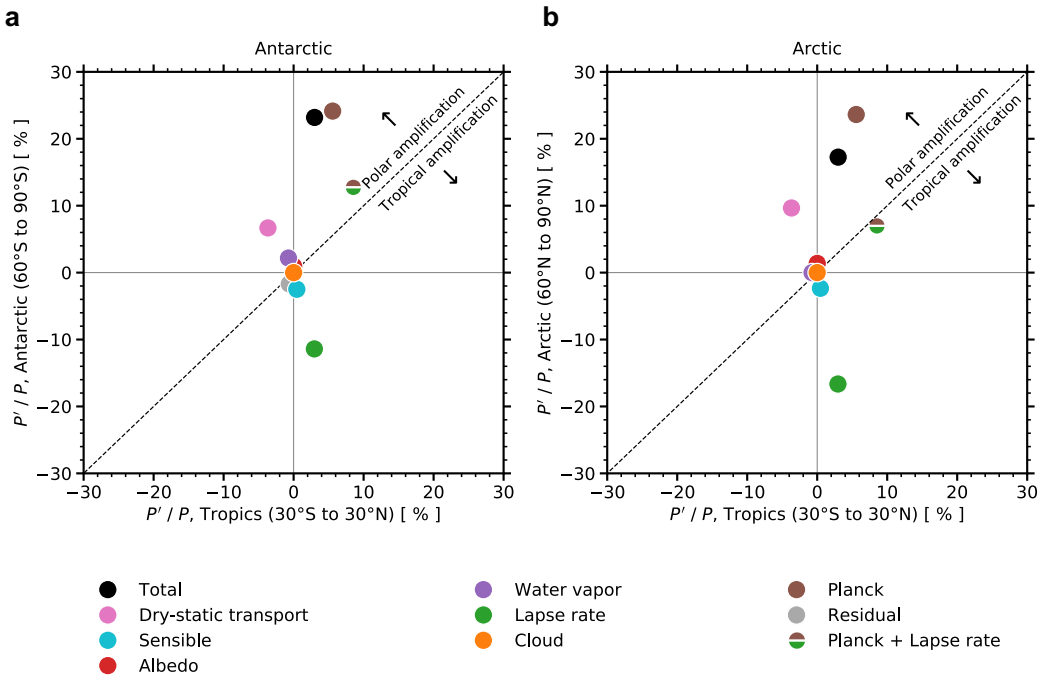

Supplemental Figure 2: **Contributions to the polar amplification of relative precipitation change.** Area-averaged multi-model mean relative precipitation change from 30°S to 30°N plotted against the area-averaged multi-model mean relative precipitation change from (a) 60°S to 90°S and (b) 60°N to 90°N. The black dot represents the total change and each colored dot represents an individual mechanism from Eq. (3) for each region in CMIP6. Changes are computed as the difference between years 130 – 150 and years 1 – 20 in abrupt-4xCO2 simulations.

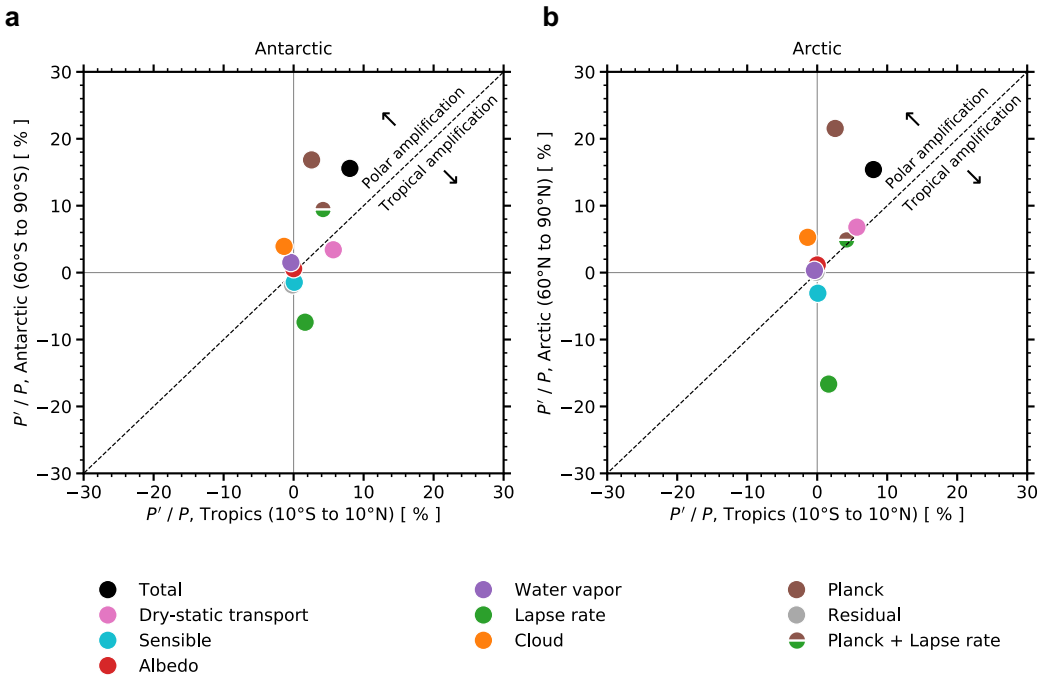

Supplemental Figure 3: **Contributions to the polar amplification of relative precipitation change.** Area-averaged multi-model mean relative precipitation change from 10°S to 10°N plotted against the area-averaged multi-model mean relative precipitation change from (a) 60°S to 90°S and (b) 60°N to 90°N. The black dot represents the total change and each colored dot represents an individual mechanism from Eq. (3) in CMIP5. Changes are computed as the difference between years 130 – 150 and years 1 – 20 in abrupt-4xCO2 simulations.

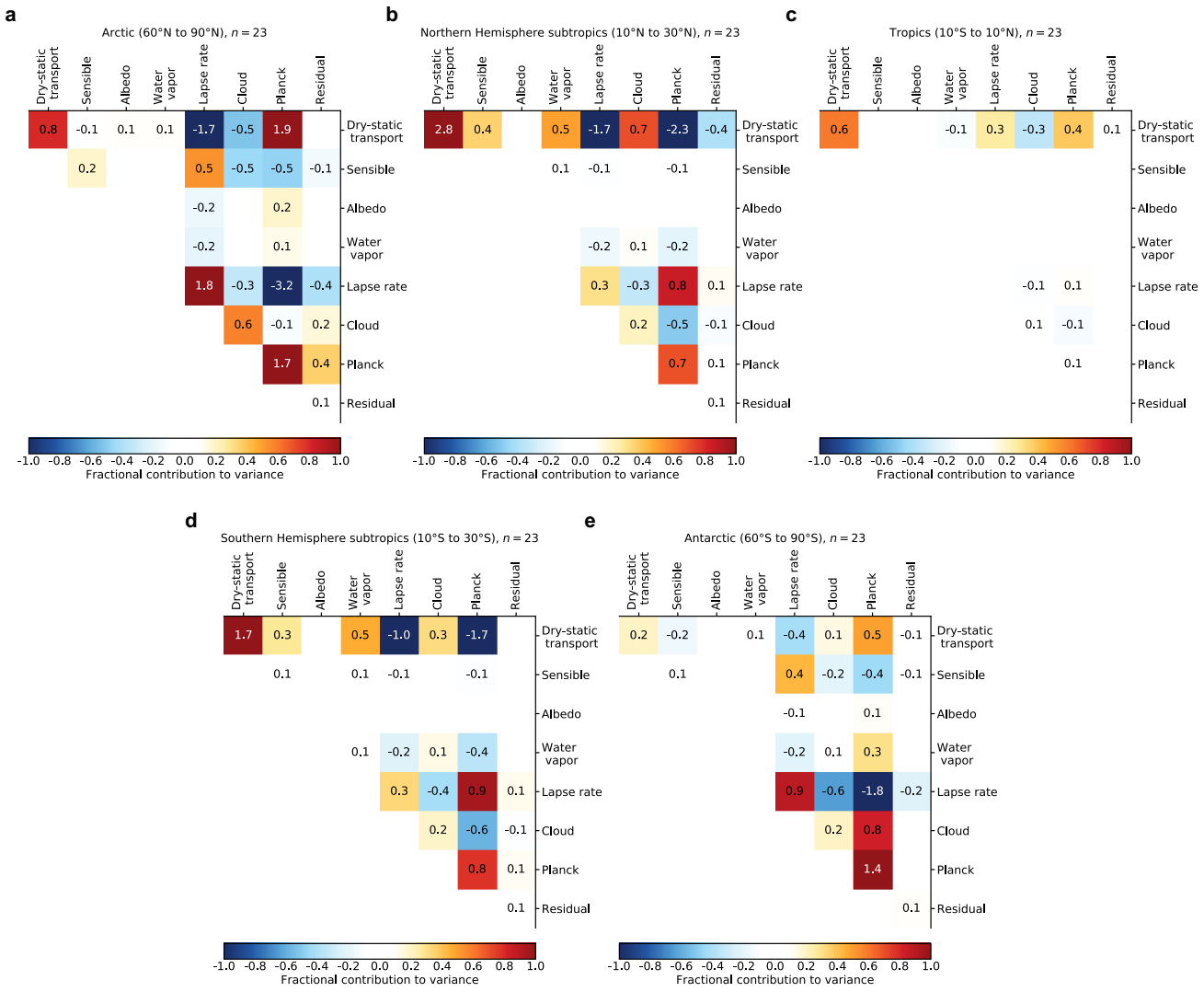

Supplemental Figure 4: **Sources of uncertainty in relative precipitation change.** Fractional contributions of each mechanism in Eq. (3) to the intermodel variance in relative precipitation change for the (a) Arctic (60°N to 90°N), (b) Northern Hemisphere subtropics (10°N to 30°N), (c) tropics (10°S to 10°N), (d) Southern Hemisphere subtropics (10°S to 30°S), and (e) Antarctic (60°S to 90°S) across CMIP5. Variances smaller than +/- 0.1 are omitted.